

A GENERALIZED CALCULATION OF THE TEMPERATURE AND DRUDE PHOTO-MODULATED OPTICAL REFLECTANCE COEFFICIENTS IN SEMICONDUCTORS

ROBERT E. WAGNER and ANDREAS MANDELIS

Photoacoustic and Photothermal Sciences Laboratory, Department of Mechanical Engineering and Ontario Laser and Lightwave Research Centre, University of Toronto, Toronto, Ontario, Canada M5S 1A4

(Received 10 August 1990; accepted in revised form 3 April 1991)

Abstract—A general calculation of the temperature and Drude reflectance coefficients, $\partial R/\partial T$ and $\partial R/\partial N$, at an optical interface, has been carried out as a means of predicting certain phenomena which may occur when the photo-modulated optical reflectance technique is employed. For instance, the effect of an inhomogeneous perturbation in the complex refractive index has been carefully examined. In addition, the value of $\Delta R/R$ has been calculated explicitly in terms of the complex refractive index at normal incidence, and the effect of a non-normal angle of incidence has been discussed. Finally, a simulation has been carried out for silicon in order to examine the various mechanisms which may affect the value of ΔR for crystalline and ion-implanted samples. Overall, this paper aims to present a detailed, consistent methodology for determining the Drude and temperature components of the photomodulated optical reflectance effect.

Keywords: Modulated reflectance, thermoreflectance, Drude effect, ion implantation, silicon.

1. INTRODUCTION

In recent years there has been considerable interest in the materials evaluation technique known as photo-modulated optical reflectance (PMOR) [1]. This technique shows promise as a means of spatially imaging the near-surface thermal and opto-electronic properties of solids, with special emphasis on semiconductors. The basis for this method is as follows: When a solid is illuminated (pumped) with intensity-modulated light, its optical properties are periodically modulated by the absorption of the incident light; for instance, the variation of the complex refractive index results in a perturbation of the sample reflectance, which can be monitored with a second (probe) beam. As Opsal *et al.* [1] have pointed out, for the super-bandgap pumping of semiconductor samples, at probe wavelengths distant from any sample 'critical points' [2], the two main mechanisms responsible for the reflectance variation are the temperature and free carrier (Drude) effects; the electric field (Franz-Keldysh) effect [2] is expected to be significant only near sample critical points, and the band-filling effect [3] is only important near the fundamental gap. Under conditions where the temperature and Drude effects dominate, the following elementary expression can be written for ΔR , the variation in optical reflectance R :

$$\Delta R = \frac{\partial R}{\partial N} \Delta N + \frac{\partial R}{\partial T} \Delta T, \quad (1)$$

or

$$\Delta R = \Delta R_N + \Delta R_T,$$

where N is the free carrier density, T is temperature, and R is a function of the complex refractive index, $\hat{n} = n + ik$, and the angle of incidence, θ .

In order to determine ΔR we must evaluate ΔT and ΔN , the periodic temperature and free carrier density fluctuations, plus $\partial R/\partial T$ and $\partial R/\partial N$, the temperature and Drude reflectance coefficients, respectively. The calculation of ΔT and ΔN is a well-established procedure, and simply involves the solution of the heat and carrier diffusion equations. Likewise, $\partial R/\partial T$ has been measured for silicon [4] at quite a few wavelengths; also, as is well known, a theoretical expression can be obtained for $\partial R/\partial N$ using the Drude model.

The calculation of ΔR is complicated somewhat by the fact that the probe beam penetrates a finite distance into the sample, within which there are inhomogeneous ΔT and ΔN fields. This problem has already been addressed by Opsal *et al.* [1], but we will provide alternate relations which facilitate numerical analysis. We will also examine the general procedure for determining $\partial R/\partial N$ and $\partial R/\partial T$, and for the first time, will graphically illustrate the effect of non-normal incidence. Finally, we will make use of the above-discussed results in order to examine the various mechanisms which can affect the value of ΔR for crystalline and ion-implanted silicon.

2. NON-UNIFORM PERTURBATION OF \hat{n}

The non-uniform perturbation of the complex refractive index stems from the fact that ΔN and ΔT are functions of depth within the sample. In order to deal with this effect, it is convenient to express $\partial R/\partial N$ and $\partial R/\partial T$ in terms of other derivatives; doing so, we obtain for ΔR :

$$\begin{aligned} \Delta R = & \left[\frac{\partial R}{\partial n} \left(\frac{\partial n}{\partial \epsilon_1} \frac{\partial \epsilon_1}{\partial N} + \frac{\partial n}{\partial \epsilon_2} \frac{\partial \epsilon_2}{\partial N} \right) \right. \\ & + \left. \frac{\partial R}{\partial k} \left(\frac{\partial k}{\partial \epsilon_1} \frac{\partial \epsilon_1}{\partial N} + \frac{\partial k}{\partial \epsilon_2} \frac{\partial \epsilon_2}{\partial N} \right) \right] \Delta N \\ & + \left[\frac{\partial R}{\partial n} \left(\frac{\partial n}{\partial \epsilon_1} \frac{\partial \epsilon_1}{\partial T} + \frac{\partial n}{\partial \epsilon_2} \frac{\partial \epsilon_2}{\partial T} \right) \right. \\ & + \left. \frac{\partial R}{\partial k} \left(\frac{\partial k}{\partial \epsilon_1} \frac{\partial \epsilon_1}{\partial T} + \frac{\partial k}{\partial \epsilon_2} \frac{\partial \epsilon_2}{\partial T} \right) \right] \Delta T, \quad (2) \end{aligned}$$

where ϵ_1 and ϵ_2 are the real and imaginary parts of the complex dielectric constant ($\hat{\epsilon}$), respectively. Later, the Drude relation for $\hat{\epsilon} = \hat{\epsilon}(N)$ will be examined, and the expression for $\partial \hat{\epsilon}/\partial N$ will be obtained. In the literature, explicit relations are often available for $n(T)$ and $k(T)$; therefore, it is useful to have relations for $\partial \epsilon_1/\partial T$ and $\partial \epsilon_2/\partial T$ in terms of $\partial n/\partial T$ and $\partial k/\partial T$:

$$\frac{\partial \epsilon_1}{\partial T} = \frac{\frac{\partial n}{\partial T} \frac{\partial k}{\partial \epsilon_2} - \frac{\partial k}{\partial T} \frac{\partial n}{\partial \epsilon_2}}{\frac{\partial n}{\partial \epsilon_1} \frac{\partial \epsilon_2} - \frac{\partial n}{\partial \epsilon_2} \frac{\partial \epsilon_1}}{\partial \epsilon_1 \partial \epsilon_2} - \frac{\partial k}{\partial \epsilon_2} \frac{\partial n}{\partial \epsilon_1}, \quad (3a)$$

and

$$\frac{\partial \epsilon_2}{\partial T} = \frac{\frac{\partial k}{\partial T} \frac{\partial n}{\partial \epsilon_1} - \frac{\partial n}{\partial T} \frac{\partial k}{\partial \epsilon_1}}{\frac{\partial n}{\partial \epsilon_1} \frac{\partial \epsilon_2} - \frac{\partial n}{\partial \epsilon_2} \frac{\partial \epsilon_1}}{\partial \epsilon_1 \partial \epsilon_2} - \frac{\partial n}{\partial \epsilon_1} \frac{\partial k}{\partial \epsilon_2}. \quad (3b)$$

Ideally, when we evaluate eqn (2) we would like to consider the situation where the probe beam does not penetrate into the sample, in which case $\Delta N = \Delta N_0$, and $\Delta T = \Delta T_0$ (the surface values). In fact, the probe beam will penetrate a finite distance into the sample, in which case we should use ($G = N$ or T):

$$\frac{\partial \epsilon_1}{\partial G} \Delta G \quad \text{and} \quad \frac{\partial \epsilon_2}{\partial G} \Delta G,$$

which represent

$$\frac{\partial \epsilon_1}{\partial G} \Delta G \quad \text{and} \quad \frac{\partial \epsilon_2}{\partial G} \Delta G$$

integrated over the penetration distance of the probe beam. Aspnes and Frova [5] present a means of evaluating:

$$\frac{\partial \epsilon_1}{\partial G} \Delta G \quad \text{and} \quad \frac{\partial \epsilon_2}{\partial G} \Delta G.$$

Specifically,

$$\begin{aligned} \frac{\partial \epsilon_1}{\partial G} \Delta G + i \frac{\partial \epsilon_2}{\partial G} \Delta G = & -i2K \int_0^x \exp(i2Kz') \\ & \times \left(\frac{\partial \epsilon_1}{\partial G} + i \frac{\partial \epsilon_2}{\partial G} \right) \Delta G(z') dz', \quad (4) \end{aligned}$$

where $K = (2\pi/\lambda)(n + ik)$, and z' is the distance into the sample. Letting $4\pi k/\lambda = \alpha$ (the absorption coefficient) and $4\pi n/\lambda = \gamma$, we can separate out the real and imaginary components of eqn (4):

$$\begin{aligned} \frac{\partial \epsilon_1}{\partial G} \Delta G = & \frac{\partial \epsilon_1}{\partial G} \int_0^x e^{-\alpha z'} \Delta G(z') [\alpha \cos(\gamma z')] \\ & + \gamma \sin(\gamma z')] dz' + \frac{\partial \epsilon_2}{\partial G} \int_0^x e^{-\alpha z'} \Delta G(z') \\ & \times [\gamma \cos(\gamma z') + \alpha \sin(\gamma z')] dz', \quad (5a) \end{aligned}$$

and

$$\begin{aligned} \frac{\partial \epsilon_2}{\partial G} \Delta G = & \frac{\partial \epsilon_2}{\partial G} \int_0^x e^{-\alpha z'} \Delta G(z') [\alpha \sin(\gamma z') \\ & - \gamma \cos(\gamma z')] dz' + \frac{\partial \epsilon_1}{\partial G} \int_0^x e^{-\alpha z'} \Delta G(z') \\ & \times [\gamma \sin(\gamma z') + \alpha \cos(\gamma z')] dz'. \quad (5b) \end{aligned}$$

If ΔG equals a constant (homogeneous perturbation), then upon evaluation of eqns (5) we find, as expected:

$$\frac{\partial \epsilon_1}{\partial G} \Delta G = \frac{\partial \epsilon_1}{\partial G} \Delta G \quad \text{and} \quad \frac{\partial \epsilon_2}{\partial G} \Delta G = \frac{\partial \epsilon_2}{\partial G} \Delta G.$$

In fact, since ΔG is generated by an optical beam, $\Delta G(z')$ is actually obtained from a solution of the heat ($G = T$) or carrier ($G = N$) diffusion equation, and for one-dimensional diffusion is expected to be of the form:

$$\Delta G(z') = \left| \sum_j \Delta G_{0,j} \exp(-\alpha_j z') \right|, \quad (6a)$$

where the α_j are the characteristic (temperature or carrier) decay parameters, and the 'absolute value' is taken because the $\Delta G_{0,j}$ can be positive or negative. For samples that are homogeneous and essentially semi-infinite in extent, the α_j are all greater than zero; for layered samples or samples of finite thickness, they can be positive or negative.

Now, one often finds that one of the $\Delta G_{0,j}$ is dominant in magnitude over the penetration distance of the probe beam; therefore,

$$\Delta G(z') \approx \Delta G_0 \exp(-\alpha_1 z'), \quad (6b)$$

where α_1 is the spatial decay parameter of the dominant term in eqn (6a). If there are several terms of similar magnitude in eqn (6a), then all of these terms should be used in eqns (5). Substituting eqn (6b) into eqns (5), and evaluating the integrals we find:

$$\overline{\frac{\partial \epsilon_1}{\partial G} \Delta G} = \frac{\partial \epsilon_1}{\partial G} \Delta G_0 \Psi_1 + \frac{\partial \epsilon_2}{\partial G} \Delta G_0 \Psi_2, \quad (7a)$$

and

$$\overline{\frac{\partial \epsilon_2}{\partial G} \Delta G} = -\frac{\partial \epsilon_1}{\partial G} \Delta G_0 \Psi_2 + \frac{\partial \epsilon_2}{\partial G} \Delta G_0 \Psi_1, \quad (7b)$$

where

$$\Psi_1 = \frac{\alpha(\alpha + \alpha_1) + \gamma^2}{(\alpha + \alpha_1)^2 + \gamma^2}, \quad (8a)$$

and

$$\Psi_2 = \frac{\gamma \alpha_1}{(\alpha + \alpha_1)^2 + \gamma^2}. \quad (8b)$$

Ψ_1 and Ψ_2 can be called 'mixing' coefficients for $\Delta \epsilon_1$ and $\Delta \epsilon_2$; they can be used to quickly ascertain the degree of mixing from a knowledge of γ , α , and α_1 , if eqn (6b) is valid. If $\gamma \gg (\alpha, \alpha_1)$ then $\Psi_1 \approx 1$, and $\Psi_2 \approx 0$. Under these conditions:

$$\overline{\frac{\partial \epsilon_1}{\partial G} \Delta G} \approx \frac{\partial \epsilon_1}{\partial G} \Delta G_0 \quad \text{and} \quad \overline{\frac{\partial \epsilon_2}{\partial G} \Delta G} \approx \frac{\partial \epsilon_2}{\partial G} \Delta G_0.$$

This limit, which is often attained experimentally, is theoretically convenient because the calculation of ΔR will only require a knowledge of the surface value of ΔG , rather than $\Delta G(z')$. Now, the question arises: how do Ψ_1 and Ψ_2 vary as a function of α_1 , for a material like germanium? For visible wavelengths ($\lambda \approx 500$ nm), the value of n for Ge is about 5; therefore, $\gamma \approx 1.3 \times 10^8 \text{ m}^{-1}$. Figure 1 shows curves for $\Psi_{1,2}$ vs α_1 , for $\alpha = 10^7 \text{ m}^{-1}$; one can see that if $\alpha_1 \ll \gamma$ then Ψ_2 is approximately zero, and there is no

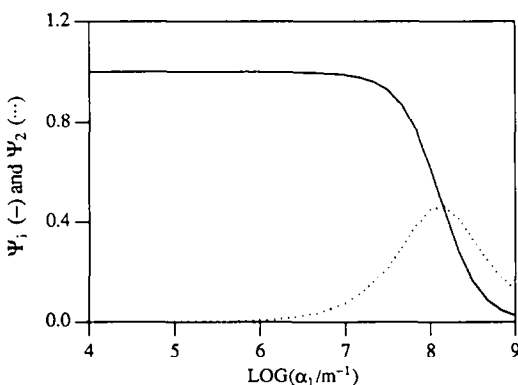


Fig. 1. Mixing coefficients (Ψ_1 and Ψ_2) vs α_1 for germanium at a probe wavelength of 500 nm. The refractive index and absorption coefficient are 5 and 10^7 m^{-1} , respectively.

mixing. On the other hand, if $\alpha_1 \gg \gamma$ then $\Psi_2 > \Psi_1$, and the magnitudes of Ψ_1 and Ψ_2 are both much less than one.

Koeppen and Handler [6] have carried out an analysis whereby they expanded $\Delta G(z)$ of eqn (4) as a Taylor series about $z = 0$, and have examined under what conditions $\Delta G(z)$ can be treated as a uniform perturbation. Our eqns (7) and (8) take this calculation one step further, and quantify the degree of mixing exactly for the case where the perturbation of ϵ is given by exponential terms, without the requirement for a Taylor expansion approximation.

Opsal *et al.* [1] have discussed certain implications of eqn (4) in order to explain some Drude PMOR results for various silicon wafers. Their method for calculating the modulated reflectance yields the same result as eqn (2), but it utilizes complex quantities, while eqn (2) allows the calculation of the modulated reflectance directly and conveniently for numerical simulations from optical parameter derivatives, without recourse to reductions of complex formulas. For instance, their relation for $\Delta R_N/R$ was obtained from:

$$\frac{\Delta R_N}{R} = \text{Re} \left[\frac{1}{\bar{R}} \frac{\partial \bar{R}}{\partial \bar{n}} \frac{\partial \bar{n}}{\partial N} \overline{\Delta N} \right], \quad (9a)$$

where $R = |\hat{R}|$, $\hat{R} = [(1 - \hat{n})/(1 + \hat{n})]^2$, Re denotes "the real part of", and:

$$\overline{\Delta N} = -i2K \int_0^\infty \exp(i2Kz') \Delta N(z') dz'. \quad (9b)$$

Those authors further went on to discuss an interesting experimental limit: consider the case where $n \gg k$ or $\gamma \gg \alpha$, and $2K\delta \ll 1$, where δ is defined in the following manner: $\Delta N = \Delta N_\delta$ for $z' < \delta$, and $\Delta N = 0$ for $z' > \delta$. These conditions would be met when the probe beam is only weakly absorbed by the sample, and $1/\delta$ is much greater than γ (a thin, surface-layer perturbation). Under these conditions eqn (4) yields:

$$\overline{\Delta \epsilon_1} = \gamma \delta \Delta G_\delta \frac{\partial \epsilon_2}{\partial G} + \alpha \delta \Delta G_\delta \frac{\partial \epsilon_1}{\partial G}$$

and

$$\overline{\Delta \epsilon_2} = -\gamma \delta \Delta G_\delta \frac{\partial \epsilon_1}{\partial G} + \alpha \delta \Delta G_\delta \frac{\partial \epsilon_2}{\partial G}.$$

This result corresponds to the mixing of $\Delta \epsilon_1$ and $\Delta \epsilon_2$ discussed by Seraphin [7].

In passing, the above example is interesting for the following reason. Since the magnitude of $\partial \epsilon_2 / \partial N$ is much less than that of $\partial \epsilon_1 / \partial N$ for crystalline materials (see the next section), the effect of having $\gamma \delta \ll 1$ (or $\gamma \ll \alpha_1$) is to reverse the sign of ΔR_N , in addition to significantly decreasing its amplitude. Similar trends may also be seen for the temperature effect, but since a universal expression is not available for $\epsilon(T)$, every material must be treated individually.

Now that we have examined some of the effects which can result from an inhomogeneous \hat{n} -perturbation, let us review the development of a general relation for $\Delta R/R$ at normal incidence, in the absence of these effects. This is a useful exercise because it is possible to ignore mixing effects with many experimental configurations.

3. CALCULATION OF $\Delta R/R$ AT NORMAL INCIDENCE (UNIFORM PERTURBATION)

At normal incidence,

$$R = \frac{(n-1)^2 + k^2}{(n+1)^2 + k^2}. \quad (10)$$

Therefore,

$$\frac{\partial R}{\partial n} = \frac{4(n^2 - k^2 - 1)}{[(n+1)^2 + k^2]^2}, \quad (11a)$$

and

$$\frac{\partial R}{\partial k} = \frac{8nk}{[(n+1)^2 + k^2]^2}. \quad (11b)$$

Now, since $\hat{n} = \epsilon^{0.5}$, we obtain:

$$k = \left[\frac{(\epsilon_1^2 + \epsilon_2^2)^{0.5} - \epsilon_1}{2} \right]^{0.5}$$

and

$$n = \left[\frac{(\epsilon_1^2 + \epsilon_2^2)^{0.5} + \epsilon_1}{2} \right]^{0.5}.$$

Therefore,

$$\frac{\partial n}{\partial \epsilon_1} = \frac{\partial k}{\partial \epsilon_1} = \frac{n}{2(n^2 + k^2)}, \quad (12a)$$

and

$$\frac{\partial n}{\partial \epsilon_2} = -\frac{\partial k}{\partial \epsilon_1} = \frac{k}{2(n^2 + k^2)}. \quad (12b)$$

At this point, the temperature component of ΔR , ΔR_T , can be easily evaluated, given $n(T)$ and $k(T)$; let us now concentrate on the carrier density effect. According to the Drude model [8, 9],

$$\epsilon_1 = \epsilon_\infty - \frac{Ne^2}{\epsilon_0} \left[\frac{1}{m_e^*} \frac{\tau_c^2}{1 + \omega^2 \tau_c^2} + \frac{1}{m_h^*} \frac{\tau_h^2}{1 + \omega^2 \tau_h^2} \right], \quad (13a)$$

and

$$\epsilon_2 = \frac{Ne^2}{\omega \epsilon_0} \left[\frac{1}{m_e^*} \frac{\tau_c}{1 + \omega^2 \tau_c^2} + \frac{1}{m_h^*} \frac{\tau_h}{1 + \omega^2 \tau_h^2} \right], \quad (13b)$$

where ϵ_∞ is the high frequency dielectric constant, m_e^* and m_h^* are the electron and hole effective masses, τ_e

and τ_h are the electron and hole relaxation times, ω is the optical radial frequency, and ϵ_0 is the permittivity of free space. (Note: mks units are used throughout.)

For crystalline materials, the carrier relaxation times are generally long enough so that $\omega \gg 1/\tau$; in this limit we obtain:

$$\frac{\partial \epsilon_1}{\partial N} = -\frac{e^2}{\epsilon_0 \omega^2} \left(\frac{1}{m_e^*} + \frac{1}{m_h^*} \right), \quad (14a)$$

and

$$\frac{\partial \epsilon_2}{\partial N} = \frac{e^2}{\epsilon_0 \omega^3} \left(\frac{1}{m_e^* \tau_e} + \frac{1}{m_h^* \tau_h} \right). \quad (14b)$$

Note that in the limit of $\omega \gg 1/\tau$, the magnitude of $\partial \epsilon_1 / \partial N$ is much greater than the magnitude of $\partial \epsilon_2 / \partial N$.

In many experimental situations with semiconductors in the visible/near-infrared region, $k \ll n$; in this case:

$$R \approx \frac{(n-1)^2}{(n+1)^2},$$

$$\frac{\partial R}{\partial n} \approx \frac{4(n-1)}{(n+1)^3} \quad \frac{\partial R}{\partial k} \approx \frac{8nk}{(n+1)^4},$$

$$\frac{\partial n}{\partial \epsilon_1} = \frac{\partial k}{\partial \epsilon_2} \approx \frac{1}{2n} \quad \frac{\partial n}{\partial \epsilon_2} = -\frac{\partial k}{\partial \epsilon_1} \approx \frac{k}{2n^2}.$$

For the Drude effect,

$$\Delta R_N \approx \frac{\partial R}{\partial n} \frac{\partial n}{\partial \epsilon_1} \frac{\partial \epsilon_1}{\partial N} \Delta N \approx -\frac{2e^2}{\epsilon_0 m \omega^2} \frac{n-1}{n(n+1)^3} \Delta N, \quad (15)$$

where $1/m = 1/m_e^* + 1/m_h^*$. Since $\omega = 2\pi c/\lambda$:

$$\Delta R_N \approx -\frac{\lambda^2 e^2}{2\pi^2 \epsilon_0 m c^2} \frac{n-1}{n(n+1)^3} \Delta N. \quad (16)$$

Overall, we obtain:

$$\frac{\Delta R_N}{R} \approx -\frac{\lambda^2 e^2}{2\pi^2 \epsilon_0 m c^2 n(n^2-1)} \Delta N. \quad (17)$$

This is the same relation obtained, in passing, by Opsal *et al.* [1]—note the change to mks units. The above detailed derivation brings out explicitly the entire set of conditions under when eqn (17) is applicable: (i) $\omega \tau \gg 1$; i.e. when probing semiconductor materials with 'high' mobility (or τ), at visible/near-i.r. frequencies; (ii) $k \ll n$ and (iii) spatial inhomogeneity effects are not important.

In the next section a simulation will be carried out in order to examine various mechanisms which can affect the value of ΔR for crystalline and ion-implanted silicon; the PMOR technique has already been used to study these types of materials [1, 10, 11], but we feel that several key points remain to be made.

We will make use of the relations presented in this section, and in section 2.

4. ΔR FOR SILICON: CRYSTALLINE AND ION-IMPLANTED SAMPLES

When a crystalline silicon substrate is ion-implanted, a surface layer is formed which is high in structural disorder [12]. As the ion dose is increased, the implant layer becomes increasingly amorphous; in fact, a heavily-implanted layer is expected to have thermal and electronic properties which are similar to those of a deposited amorphous layer. In this simulation, a heavily-implanted layer will be examined which is effectively amorphous. A layer which is implanted to a moderate degree, and which is not completely amorphous, would be expected to yield a behaviour intermediate to those of the crystalline and heavily-implanted systems. Since the PMOR technique has been applied to the characterization of implanted materials [13, 14], it would be useful to examine how the value of ΔR is expected to vary as the implantation dose is increased. There will be some uncertainty in the temperature component due to the fact that there is no available information regarding the value of $\partial\epsilon_1/\partial T$ and $\partial\epsilon_2/\partial T$ for implanted or amorphous materials.

In order to calculate ΔR with mixing effects included, one must obtain the depth-profiles of ΔN and ΔT for the given excitation conditions. Although calculational difficulty is reduced considerably when the carrier and heat diffusion equations are solved in the one-dimensional limit, in order to reflect current experimental practice we have solved these equations in the three-dimensional limit [15], which is necessary when tightly-focussed Gaussian laser beams are used to excite a sample. Since our calculations involved a numerical Hankel transform, mixing effects could not be determined analytically; these effects were quantified as follows. For a given set of simulation parameters, ΔG ($G = N, T$) was calculated numerically and then plotted as a function of z , over the penetration distance of the probing beam. In most cases, the $\Delta G(z)$ profile was well-approximated by a single exponential term, such as given by eqn (6b); the decay parameter, α_1 , could then be obtained from the graphical representation of $\Delta G(z)$, and used to determine the mixing coefficients.

Calculations were carried out at two modulation frequencies, 10^3 and 10^6 Hz; furthermore, the pump beam was chosen to have a $1/e$ beam waist diameter of $1 \mu\text{m}$, which reflects the diffraction-limited spot size of a visible beam. The crystalline sample was modelled as a semi-infinite slab, while the implanted sample was considered to be a thin layer on a semi-infinite substrate.

Now, let us denote ΔR for the crystalline and implanted/amorphous materials as ΔR_c and ΔR_a , respectively. Also, assume that electrons and holes have the same average order-of-magnitude mobility

(μ), relaxation time (τ), and effective mass (m^*)—an adequate assumption for this simulation. Finally, the pump and probe wavelengths match those of earlier reports [1, 10, 11, 13, 14]; the pump is at 488 nm (2.55 eV), and the probe is at 632.8 nm (1.96 eV).

In the next two subsections, the Drude and temperature components of ΔR will be examined separately.

4.1. The Drude component of ΔR

In order to determine $\partial\epsilon/\partial N$, one must know the carrier mobility so that the scattering relaxation time can be calculated. The crystalline Si is assumed to have a mobility of $0.08 \text{ m}^2 \text{ V}^{-1} \text{ s}^{-1}$, an average value for electrons and holes in a high-quality substrate [16]. The implanted layer is effectively amorphous (unannealed) and has a thickness of $0.3 \mu\text{m}$; Christofides *et al.* [12] have performed various electronic measurements on such a layer (arsenic implant, dose = $8 \times 10^{14} \text{ cm}^{-2}$, energy = 120 keV) and found the Hall mobility to be around $10^{-3} \text{ m}^2 \text{ V}^{-1} \text{ s}^{-1}$. This value corresponds well with the electron extended-state mobility reported for *a*-Si:H in a review by Dresner [17].

In order to obtain the carrier density profiles in the two silicon samples, one must know the carrier diffusion coefficients, carrier lifetimes, and interface recombination velocities. The carrier diffusion coefficients (D) can be obtained from the carrier mobilities via the Einstein relation [16]; for the crystalline material, $D \approx 2 \times 10^{-3} \text{ m}^2 \text{ s}^{-1}$, and for the implanted material, $D \approx 2.6 \times 10^{-5} \text{ m}^2 \text{ s}^{-1}$. With regard to the carrier lifetimes, for the implanted/amorphous sample the recombination time is replaced by the trapping time, which provides an indication as to how long it takes the free, photo-generated carriers to be trapped in localized bandedge defect states. In general, it is much more difficult to model carrier diffusion in defect materials owing to the complex nature of the localized 'bandgap' states. Now, for the crystalline material, the carrier lifetime can be as high as 10^{-5} s [16], while in the implanted material 10^{-12} s is a typical value [18]. Finally, we will assume that all surface/interface recombination velocities are zero, since this parameter can vary over a considerable range depending upon sample preparation methods.

Using the above-quoted values for the carrier mobility, the free-carrier scattering relaxation times, τ , can be calculated using the following relation [16]:

$$\tau = \frac{\mu m^*}{e}, \quad (18)$$

where e is the electronic charge. Letting $m^* = 0.2 m_0$ [16], where m_0 is the free-electron mass, and $\tau_e \approx \tau_h \equiv \tau$, we can now calculate τ for the two materials:

$$\tau_c = 9.11 \times 10^{-14} \text{ s} \quad \text{and} \quad \tau_a = 1.14 \times 10^{-15} \text{ s}.$$

Rewriting eqn (13), and differentiating with respect to N , we obtain:

$$\frac{\partial \epsilon_1}{\partial N} = -\eta \frac{\tau^2}{1 + \omega^2 \tau^2}, \quad (19a)$$

and

$$\frac{\partial \epsilon_2}{\partial N} = \eta \frac{\tau}{\omega(1 + \omega^2 \tau^2)}, \quad (19b)$$

where $\eta = 2e^2/\epsilon_0 m^*$. At 632.8 nm, $\omega = 3 \times 10^{15}$ rad s⁻¹; using the values of τ shown above, we can evaluate eqns (19) for the two materials:

$$[\partial \epsilon_1 / \partial N]_c = -1.1 \times 10^{-31} \eta$$

$$[\partial \epsilon_2 / \partial N]_c = 4.1 \times 10^{-34} \eta,$$

$$[\partial \epsilon_1 / \partial N]_a = -1.0 \times 10^{-31} \eta$$

$$[\partial \epsilon_2 / \partial N]_a = 3.0 \times 10^{-32} \eta.$$

Note that for both samples $|\partial \epsilon_1 / \partial N|$ is greater than $|\partial \epsilon_2 / \partial N|$.

Now, α_1 was obtained at 10³ and 10⁶ Hz for the crystalline and implanted samples, using the graphical method and the parameters detailed earlier in this section. The absorption coefficient for the pump beam, α_g , is given in Table 1, along with the optical parameters (α , k , γ and n) of the two samples at the probe wavelength; note that for the implanted/amorphous sample, the values in Table 1 are those for *a*-Si, taken from Ley [20]. Figure 2 shows the natural logarithm of the carrier density modulation vs distance into the crystalline sample; these data are adequately described by a straight line ($\alpha_1 = 8.0 \times 10^5$ m⁻¹), but note that the slope goes to zero at the surface ($z = 0$) because the boundary condition requires that the carrier density gradient be zero there. Figure 3 shows a similar graph for the implanted sample ($\alpha_1 = 7.6 \times 10^7$ m⁻¹). Since the carrier density profiles were found to be identical at 10³ and 10⁶ Hz, we will no longer refer to modulation frequency in our discussion of the Drude mechanism.

Using the α_1 data quoted above, Table 1, and eqns (8), values for $\Psi_{1,2}$ can be calculated for the two samples:

$$[\Psi_1]_{N,c} = 1.0 \quad [\Psi_2]_{N,c} = 0.0,$$

$$[\Psi_1]_{N,a} = 0.52 \quad [\Psi_2]_{N,a} = 0.44.$$

Table 1. Dielectric parameters for various silicon samples. Wavelengths—pump: 488 nm; probe: 632.8 nm

	Crystalline [16, 19]	Implanted/amorphous [20]
α_g (m ⁻¹)	2×10^6	3×10^7
α (m ⁻¹)	4.5×10^5	10^7
k	0.023	0.50
γ (m ⁻¹)	7.7×10^7	7.9×10^7
n	3.9	4.0

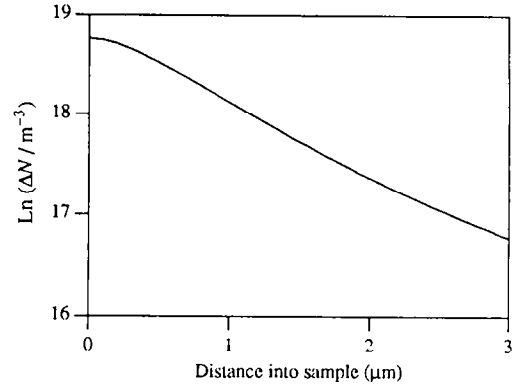


Fig. 2. $\text{Ln}(\Delta N/\text{m}^{-3})$ vs distance into sample (μm), over penetration distance of probe beam ($\lambda = 632.8$ nm), for crystalline silicon. The photon rate is one per second. $\alpha_1 = 8.0 \times 10^5$ m⁻¹. See text for simulation parameters.

Now, using eqns (7), we obtain:

$$[\overline{\Delta \epsilon_1}]_{N,c} = -1.1 \times 10^{-31} \eta \Delta N_{0,c}$$

$$[\overline{\Delta \epsilon_2}]_{N,c} = 4.1 \times 10^{-34} \eta \Delta N_{0,c},$$

$$[\overline{\Delta \epsilon_1}]_{N,a} = -3.9 \times 10^{-32} \eta \Delta N_{0,a}$$

$$[\overline{\Delta \epsilon_2}]_{N,a} = 6.0 \times 10^{-32} \eta \Delta N_{0,a}.$$

Overall, using eqn (2) we get:

$$\Delta R_{N,c} = -1.4 \times 10^{-33} \eta \Delta N_{0,c}$$

and

$$\Delta R_{N,a} = -1.6 \times 10^{-34} \eta \Delta N_{0,a}.$$

Note that eqn (15) gives a value of $-1.4 \times 10^{-33} \eta \Delta N_0$ for ΔR_N . We can draw the following conclusions from the above results: eqn (15) appears to provide an accurate approximation for evaluating ΔR_N for the crystalline silicon, but may be off by an order of magnitude for the ion-implanted silicon, given the parameters of this particular simulation. For the crystalline sample, carrier diffusion tends to

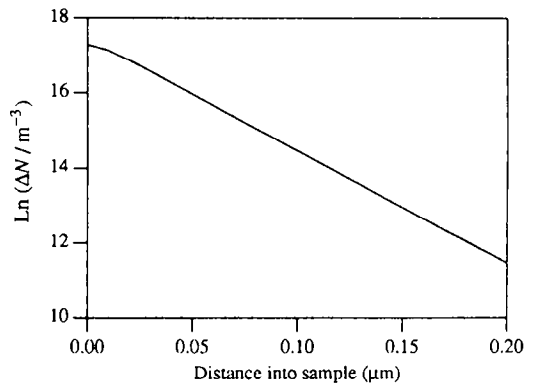


Fig. 3. $\text{Ln}(\Delta N/\text{m}^{-3})$ vs distance into sample (μm), over penetration distance of probe beam ($\lambda = 632.8$ nm), for implanted silicon. The photon rate is one per second. $\alpha_1 = 7.6 \times 10^7$ m⁻¹. See text for simulation parameters.

minimize the refractive index inhomogeneity, and thus, any mixing effects (see eqns (7)).

As a final means of examining the variation of ΔR_N , ΔN_0 was calculated for the two samples; we obtained:

$$\Delta N_{0,c} = 2.2 \times 10^8 I_0 \quad \text{and} \quad \Delta N_{0,a} = 3.3 \times 10^7 I_0,$$

where I_0 is the number of photons per second in the beam. Overall, using $\eta = 3.17 \times 10^4$ mks units, we obtain for ΔR_N :

$$\begin{aligned} \Delta R_{N,c} &= -9.8 \times 10^{-21} I_0 \\ \text{and } \Delta R_{N,a} &= -1.7 \times 10^{-22} I_0. \end{aligned} \quad (20)$$

The above values for ΔR_N indicate that the very short trapping time and dielectric constant mixing in the heavily-implanted silicon reduce the magnitude of ΔR_N to a level about 58 times below that for the crystalline sample.

Carrier effects in the implanted/amorphous material are complicated by the fact that although non-equilibrium carriers are quickly trapped in localized bandedge tail-states ($< 10^{-12}$ s), they can persist in the localized states for quite a long time before recombining. During this time the trapped carriers can be emitted into the extended band states, and re-captured, many times. If the carriers present in the localized states perturb the sample dielectric constant, there may be a significant non-Drude carrier-related reflectance modulation mechanism in implanted/amorphous silicon. For instance, bandfilling or electric-field effects (see Introduction) may be significant in this case.

The above simulation has been performed in order to illustrate how the various terms which are used to evaluate ΔR_N (Drude effect) are expected to vary for two types of technologically important silicon. Obviously, an accurate knowledge of the various optical and transport parameters is required if the value of ΔR_N is to be predicted with any confidence for a given sample. The simulation has brought out the following facts. First, due to the usual increase in the absorption coefficient and the decrease in the carrier diffusion length as the amount of disorder is increased, the effects of inhomogeneity are greatest in disordered materials. Second, increasing the amount of disorder tends to push the magnitude of $\partial R/\partial N$ downward. Finally, ΔN is reduced in defect-rich material due to the short trapping time, reducing ΔR_N .

Now that the Drude component of ΔR has been examined, let us determine how the temperature component is expected to vary for the two silicon samples.

4.2. The temperature component of ΔR

The first step in determining ΔR_T is to evaluate eqn (3) for $\partial \epsilon_1/\partial T$ and $\partial \epsilon_2/\partial T$. The values for $\partial n/\partial T$

and $\partial k/\partial T$ have been measured for crystalline silicon: $\partial n/\partial T \approx 6 \times 10^{-4}$ [4], and $\partial k/\partial T \approx 1.5 \times 10^{-4}$ [21]. Evaluating eqn (3) for the optical parameters listed in Table 1, we obtain:

$$[\partial \epsilon_1/\partial T]_c = 4.7 \times 10^{-3} \quad [\partial \epsilon_2/\partial T]_c = 1.2 \times 10^{-3},$$

$$[\partial \epsilon_1/\partial T]_a = 4.6 \times 10^{-3} \quad [\partial \epsilon_2/\partial T]_a = 1.8 \times 10^{-3}.$$

Note that $\partial n/\partial T$ and $\partial k/\partial T$ were assumed to be sample independent.

In order to obtain temperature depth-profiles, one must have a knowledge of both the electronic and thermal properties of the samples. The electronic properties of the sample and the excitation conditions were given in section 4.1; the thermal properties of the two samples are as follows. For the crystalline silicon [22], the thermal diffusivity is $\beta_s = 9.2 \times 10^{-5} \text{ m}^2 \text{ s}^{-1}$, and the thermal conductivity is $k_s = 148 \text{ W m}^{-1} \text{ K}^{-1}$. Assuming that the implanted layer has thermal properties similar to those of amorphous silicon, we obtain $k_s = 2 \text{ W m}^{-1} \text{ K}^{-1}$ [23]; also, if the implanted layer has the same specific heat and density as the crystalline sample, we obtain a thermal diffusivity of: $\beta_s = 1.2 \times 10^{-6} \text{ m}^2 \text{ s}^{-1}$.

Using the method outlined in Ref. 15, the temperature profiles were obtained for the two samples at 10^3 and 10^6 Hz. Figure 4 shows the ΔT profile for the crystalline material at 10^6 Hz ($\alpha_1 = 7.2 \times 10^5 \text{ m}^{-1}$); the curve at 10^3 Hz was within a few per cent of being identical. Figure 5 shows the ΔT profile for the implanted sample at 10^6 Hz. In this case ΔT is not very well-described by an exponential term; keeping this reservation in mind, fitting a straight line to the data of Fig. 5 yields $\alpha_1 = 5.3 \times 10^6 \text{ m}^{-1}$.

We can now evaluate the Ψ for the two samples. Using the parameters of Table 1 and the values of α_1 quoted above, we obtain: $\Psi_1 = 1$, and $\Psi_2 = 0$ (crystalline sample), and $\Psi_1 = 0.99$, and $\Psi_2 = 0.06$ (implanted sample). In other words, mixing effects can be neglected for the thermal component of the

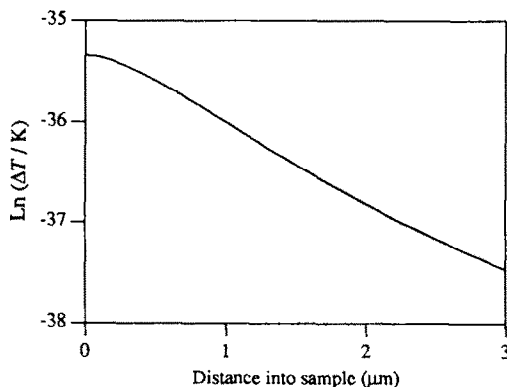


Fig. 4. $\text{Ln}(\Delta T/\text{K})$ vs distance into sample (μm), over penetration distance of probe beam ($\lambda = 632.8 \text{ nm}$), for crystalline silicon. The photon rate is one per second. The modulation frequency is 10^6 Hz. $\alpha_1 = 7.2 \times 10^5 \text{ m}^{-1}$. See text for other simulation parameters.

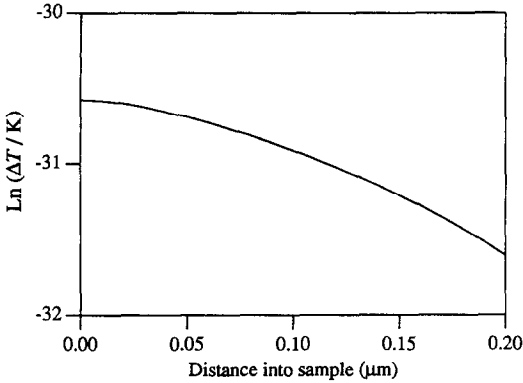


Fig. 5. $\text{Ln}(\Delta T/\text{K})$ vs distance into sample (μm), over penetration distance of probe beam ($\lambda = 632.8 \text{ nm}$), for implanted silicon. The photon rate is one per second. The modulation frequency is 10^6 Hz . $\alpha_1 = 5.3 \times 10^6 \text{ m}^{-1}$. See text for other simulation parameters.

signal. Therefore, $[\overline{\Delta\epsilon_i}]_{\text{T}} \approx [\Delta\epsilon_i]_{\text{T}}$, for $i = 1, 2$, for both samples. Now, using eqns (7) we obtain:

$$[\overline{\Delta\epsilon_1}]_{\text{T,c}} = 4.7 \times 10^{-3} \Delta T_{0,c}$$

$$[\overline{\Delta\epsilon_2}]_{\text{T,c}} = 1.2 \times 10^{-3} \Delta T_{0,c}$$

$$[\overline{\Delta\epsilon_1}]_{\text{T,a}} = 4.6 \times 10^{-3} \Delta T_{0,a}$$

$$[\overline{\Delta\epsilon_2}]_{\text{T,a}} = 1.8 \times 10^{-3} \Delta T_{0,a}$$

Overall, using eqn (2) we get:

$$\Delta R_{\text{T}} = 5.9 \times 10^{-5} \Delta T_{0,c}$$

Going farther, ΔT_0 was evaluated for the samples using the electronic and thermal transport parameters quoted in this section; the modulation frequency was 10^6 Hz , and the pump beam waist ($1/e$) was $1 \mu\text{m}$ (almost identical values were obtained at 10^3 Hz). For the crystalline sample we found $\Delta T_0 = 4.3 \times 10^{-16} I_0$, and the implanted sample yielded a value which was 100 times larger. Let us now concentrate on the crystalline sample, since its thermal and optical properties are well known. Using the above value of ΔT_0 , we obtain:

$$\Delta R_{\text{T,c}} = 2.6 \times 10^{-20} I_0$$

Now, consider a pump beam which provides 20 mW of absorbed optical power to the sample, and is focussed to a beam waist diameter of $1 \mu\text{m}$; this corresponds to a photon rate (I_0) of 4.9×10^{16} photons s^{-1} . In this case we obtain the following values for ΔR , for the crystalline sample:

$$\Delta R_{\text{N}} = -3.0 \times 10^{-4} \quad \Delta R_{\text{T}} = 1.3 \times 10^{-3}$$

where ΔR_{N} was evaluated via eqn (20). It appears that the magnitudes of ΔR_{N} and ΔR_{T} are quite similar for crystalline silicon, in agreement with the results of

Opsal *et al.* [1]. Note that in order to determine the total ΔR , one must remember that ΔR_{N} and ΔR_{T} are added like vectors, because ΔN and ΔT have both a magnitude, and a phase lag relative to the periodically modulated pump beam.

Several observations can be made regarding the temperature component of the modulation signal calculated in this simulation. First, the value of ΔT_0 may be two orders of magnitude greater in the heavily-implanted silicon, due to the small value of the thermal conductivity in that material. Since we do not know the value of $\partial R/\partial T$ for the implanted sample, it is difficult to predict the actual magnitude of ΔR_{T} in the implanted sample.

With regard to the relative magnitude of ΔR_{N} and ΔR_{T} , it appears that under most excitation/probing conditions (visible light) for crystalline silicon, $|\Delta R_{\text{T}}| > |\Delta R_{\text{N}}|$. For implanted silicon, it appears that $|\Delta R_{\text{T}}|$ should increase with dose, due to the increase in ΔT_0 , although the variation in $\partial R/\partial T$ with dose (at 632.8 nm) is unknown at present. For the Drude component in the implanted silicon, one would expect this component to be less important than in the crystalline sample. It should be noted that this simulation is limited considerably by a lack of knowledge regarding the actual physical processes occurring in the implanted silicon. Several material parameters are not well known, and the actual reflectance modulation mechanisms may be somewhat different than for crystalline silicon.

Now, as a final calculation let us examine whether the presence of an oblique incidence probe beam is of any consequence in determining the value of ΔR .

5. MODULATED REFLECTANCE AT OBLIQUE ANGLES OF INCIDENCE

In 1967, Fischer and Seraphin [24] presented a set of relations which allow one to calculate $\Delta R/R$ at oblique angles of incidence. Although they discussed various effects induced by an oblique-incidence probe beam, they never showed how $\partial R/\partial G$ ($G = N, T$) is

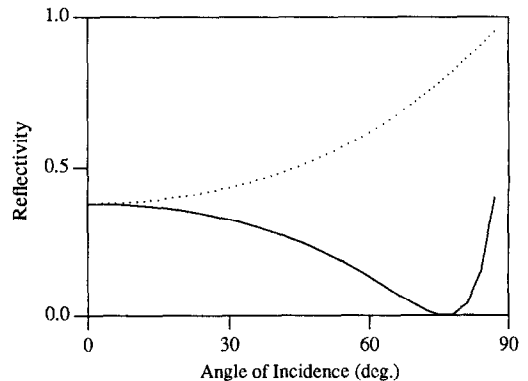


Fig. 6. Reflectivity for s - and p -polarized light (R_s : dotted line, R_p : solid line) vs angle of incidence, for an air/silicon interface. The photon energy is 2.4 eV ; $\epsilon_1 = 17.76$ and $\epsilon_2 = 0.508$.

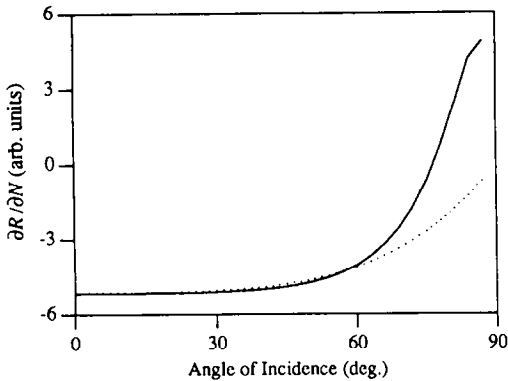


Fig. 7. $\partial R/\partial N$ (*s*-polarized: dotted line, *p*-polarized: solid line) vs angle of incidence, for an air/silicon interface. See Fig. 6 for sample parameters.

expected to vary, for *p*- and *s*-polarized beams, over the full range of angles from 0 to 90 deg. We have calculated $\partial R/\partial G$ by our own method, and have obtained results comparable to those predicted by eqns (2)–(6) of Ref. 24. We will illustrate this behavior by examining the angular dependence of $\partial R/\partial N$; $\partial R/\partial T$ would yield a similar behavior.

Now, Fig. 6 shows R_s and R_p vs θ for an air/silicon interface ($h\nu = 2.4$ eV; $\epsilon_1 = 17.76$, $\epsilon_2 = 0.508$). The *p*-polarized light shows the familiar Brewster angle (θ_B) phenomenon where $R_p \approx 0$ near 76 deg.

Figure 7 shows $\partial R_s/\partial N$ and $\partial R_p/\partial N$ vs θ for the same air/silicon interface. For *s*-polarized light, $\partial R_s/\partial N$ decreases in magnitude as θ is increased; for the *p*-polarized light, $\partial R_p/\partial N$ is initially negative and then becomes positive for $\theta > \theta_B$.

Finally, Fig. 8 depicts $(1/R)\partial R/\partial N$ for *s*- and *p*-polarized light. Note that for *p*-polarized light, a large magnitude is obtained near θ_B due to the vanishing of R_p .

The following conclusions can be drawn from Figs 6–8. $\partial R/\partial N$ is fairly insensitive to θ for $\theta < 50$ deg. For $\theta > 60$ deg, $\partial R_p/\partial N$ is more sensitive to changes in θ than $\partial R_s/\partial N$. Also, for both *s*- and *p*-polarized light, $\partial R/\partial N$ is largest at normal

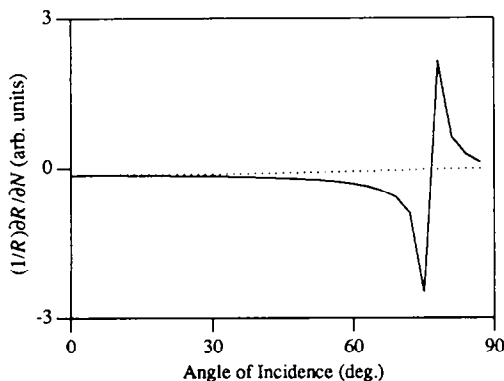


Fig. 8. $(1/R)\partial R/\partial N$ (*s*-polarized: dotted line, *p*-polarized: solid line) vs angle of incidence, for an air/silicon interface. See Fig. 6 for sample parameters.

incidence, although $\partial R_p/\partial N$ is also large near $\theta = 90$ deg (experimentally impractical). Overall, there are no real experimental benefits to be obtained by choosing $\theta > 50$ deg.

6. CONCLUSIONS

With regard to the non-uniform perturbation of \hat{n} , generalized explicit expressions for $\overline{\Delta\epsilon_1}$ and $\overline{\Delta\epsilon_2}$ have been obtained, for general carrier and temperature profiles. A pair of mixing coefficients, Ψ_1 and Ψ_2 , have been defined, which characterize the degree to which $\Delta\epsilon_1$ and $\Delta\epsilon_2$ are interchanged; these mixing coefficients effectively illustrate how inhomogeneity effects vary as the unperturbed optical parameters of the sample and the spatial profile of the dielectric constant perturbation are varied. Our treatment of this problem is consistent with that of Aspnes and Froya [5].

A detailed calculation of $\Delta R/R$ at normal incidence, for arbitrary n and k , has also been given. In addition, the behavior of $\Delta R/R$ as a function of incidence angle was examined, and ΔR was found to be largest at normal incidence, with no dramatic variations for incidence below 50 deg.

Finally, a simulation was carried out in order to examine the value of ΔR for crystalline and heavily-implanted/amorphous silicon; the simulation parameters were chosen to reflect current experimental practice. When carrier diffusion effects were taken into account, the value of ΔR_N for the crystalline sample was found to be accurately given by the approximate relation eqn (15). The carrier density gradient in the crystalline sample was found to be decreased by diffusion into the bulk, decreasing the inhomogeneity in ΔN . When the carrier diffusion equation was solved for the implanted sample, a larger carrier density gradient was obtained, resulting in a significant mixing of $\Delta\epsilon_1$ and $\Delta\epsilon_2$; thus, eqn (15) was found to be inadequate for the implanted sample. Also, the smaller value of ΔN_0 in the implanted sample relative to the crystalline sample resulted in a smaller value for ΔR_N . With regard to the temperature component, the value of ΔR_T was found to be considerably larger in the implanted sample, but the sample variation in $\partial R/\partial T$ was not included.

It should be easiest to interpret experimental data for high-quality crystalline samples, while samples with disordered bulk or surface regions may be more difficult to model, owing to inhomogeneity effects and complex carrier diffusion and recombination dynamics. This work has shown that the Drude component of ΔR is expected to be very sensitive to changes in the electronic transport properties of a material, while the temperature component is sensitive to both the electronic and thermal transport properties. Both components of ΔR can vary considerably when a crystalline sample is ion-implanted.

Overall, for the first time in one paper, we discuss all of the issues regarding the evaluation of ΔR_N and

ΔR_T for a semiconductor material, short of presenting an exhaustive set of solutions for the three-dimensional diffusion equations; this particular aspect of the problem will be dealt with in a future paper. The detailed and consistent methodology presented in this work, along with the complete set of mathematical relationships required to calculate the modulated reflectance, should minimize the amount of effort required for future theoretical modelling.

Acknowledgements—The authors wish to acknowledge the support of the Ontario Laser and Lightwave Research Centre (OLLRC) and of the Natural Sciences and Engineering Research Council of Canada (NSERC) throughout this work.

REFERENCES

- Opsal J., Taylor M. W., Smith W. L. and Rosencwaig A., *J. appl. Phys.* **61**, 240 (1987).
- Aspnes D. E. and Bottka N., in *Semiconductors and Semimetals*, Vol. 9 (Edited by R. K. Willardson and A. C. Beer), p. 457. Academic Press, New York (1972).
- Gay J. G. and Klauder L. T., Jr., *Phys. Rev.* **172**, 811 (1968).
- Jellison G. E., Jr. and Burke H. H., *J. appl. Phys.* **60**, 841 (1986).
- Aspnes D. E. and Frova A., *Solid St. Commun.* **7**, 155 (1968).
- Koepfen S. and Handler P., *Phys. Rev.* **187**, 1182 (1969).
- Seraphin B. O. in *Semiconductors and Semimetals*, Vol. 9 (Edited by R. K. Willardson and A. C. Beer), pp. 16–17. Academic Press, New York (1972).
- Carver G. E. and Michalski J. D., *Proc. SPIE* **794**, 152 (1987).
- Harrison W. A., *Solid State Theory*, p. 287. Dover, New York (1979).
- Christofides C., Vitkin I. A. and Mandelis A., *J. appl. Phys.* **67**, 2815 (1990).
- Vitkin I. A., Christofides C. and Mandelis A., *J. appl. Phys.* **67**, 2822 (1990).
- Christofides C., Jaouen H. and Ghibaudo G., *J. appl. Phys.* **65**, 4832 (1989).
- Smith W. L., Rosencwaig A. and Willenborg D. L., *Appl. Phys. Lett.* **47**, 584 (1985).
- Smith W. L., Powell R. A. and Woodhouse J. D., *Proc. SPIE* **530**, 188 (1985).
- McDonald F. A., Guidotti D. and DelGiudice T. M., in *Review of Progress in Quantitative Nondestructive Evaluation*, 6B (Edited by D. O. Thompson and D. E. Chimenti), p. 1361. Plenum, New York (1987).
- Fahrenbruch A. L. and Bube R. H., *Fundamentals of Solar Cells*. Academic Press, New York (1983).
- Dresner J., in *Semiconductors and Semimetals*, Vol. 21, Part C (Edited by R. K. Willardson and A. C. Beer, volume edited by J. I. Pankove), p. 203. Academic Press, New York (1984).
- Doany F. E., Grichkowsky D. and Chi C. C., *Appl. Phys. Lett.* **50**, 460 (1987).
- Aspnes D. E. and Studna A. A., *Phys. Rev.* **B27**, 985 (1983).
- Ley L., in *The Physics of Hydrogenated Amorphous Silicon II, Topics in Applied Physics*, Vol. 56 (Edited by J. D. Joannopoulos and G. Lucovsky), pp. 141–157. Springer-Verlag, Berlin (1984).
- Jellison G. E., Jr. and Modine F. A., *Appl. Phys. Lett.* **41**, 180 (1982).
- Silicon data sheet, Exotic Materials, Inc., Costa Mesa, CA (1972).
- Goldsmid H. J., Kaila M. M. and Paul G. L., *Phys. Status Solidi* **A76**, K31 (1983).
- Fischer J. E. and Seraphin B. O., *Solid St. Commun.* **5**, 973 (1967).